Donor B-cell alloantibody deposition and germinal center formation are required for the development of murine chronic GVHD and bronchiolitis obliterans

Mathangi Srinivasan,[1] Ryan Flynn,[1] Andrew Price,[1] Ann Ranger,[2] Jeffrey L. Browning,[2] Patricia A. Taylor,[1] Jerome Ritz,[3] Joseph H. Antin,[3] William J. Murphy,[4] Leo Luznik,[5] Mark J. Shlomchik,[6] *Angela Panoskaltsis-Mortari,[1] and *Bruce R. Blazar[1]

[1]Masonic Cancer Center and Department of Pediatrics, Division of Blood and Marrow Transplantation, University of Minnesota, Minneapolis, MN; [2]Department of Immunobiology, Biogen Idec, Cambridge, MA; [3]Dana-Farber Cancer Institute and Brigham and Women's Hospital, Boston, MA; [4]Department of Dermatology, University of California–Davis Cancer Center and School of Medicine, Sacramento, CA; [5]Sidney Kimmel Comprehensive Cancer Center and Department of Oncology, Johns Hopkins University School of Medicine, Baltimore, MD; and [6]Departments of Immunobiology and Laboratory Medicine, Yale University School of Medicine, New Haven, CT

Chronic GVHD (cGVHD) poses a significant risk for HSCT patients. Preclinical development of new therapeutic modalities has been hindered by models with pathologic findings that may not simulate the development of human cGVHD. Previously, we have demonstrated that cGVHD induced by allogeneic HSCT after a conditioning regimen of cyclophosphamide and total-body radiation results in pulmonary dysfunction and airway obliteration, which leads to bronchiolitis obliterans (BO), which is pathognomonic for cGVHD of the lung. We now report cGVHD manifestations in a wide spectrum of target organs, including those with mucosal surfaces. Fibrosis was demonstrated in the lung and liver and was associated with CD4$^+$ T cells and B220$^+$ B-cell infiltration and alloantibody deposition. Donor bone marrow obtained from mice incapable of secreting IgG alloantibody resulted in less BO and cGVHD. Robust germinal center reactions were present at the time of cGVHD disease initiation. Blockade of germinal center formation with a lymphotoxin-receptor–immunoglobulin fusion protein suppressed cGVHD and BO. We conclude that cGVHD is caused in part by alloantibody secretion, which is associated with fibrosis and cGVHD manifestations including BO, and that treatment with a lymphotoxin-β receptor–immunoglobulin fusion protein could be beneficial for cGVHD prevention and therapy. (*Blood*. 2012;119(6):1570-1580)

Introduction

Chronic GVHD (cGVHD) is a significant complication of allogeneic HSCT.[1] Progress in developing interventional strategies to counter cGVHD has been hampered by variable onset and pathologic manifestations of cGVHD, now better defined by the National Institutes of Health consensus conference,[2] and a dearth of robust preclinical venues that closely mimic conditions in which cGVHD is generated and manifested.[3]

Although the exact causes of cGVHD are unknown, higher antibody levels have been associated with autoimmunity and implicated in cGVHD.[4,5] Studies of newly diagnosed patients with extensive cGVHD showed that they had elevated soluble B-cell activating factor (BAFF) levels and anti-ds-DNA antibodies.[6,7] Increased soluble BAFF in cGVHD was associated with higher circulating levels of pre–germinal center (GC) B cells and post-GC plasmablasts.[8] B cells from cGVHD patients are hyperresponsive to TLR-9 signaling and have up-regulated CD86 levels,[9] which suggests an important participatory role for B cells in establishing cGVHD and emphasizes the need for further investigation into the immunologic role of B cells in cGVHD pathogenesis.

Existing murine cGVHD models simulate one or more of the pathologic manifestations, such as increased serum antibodies (typically anti-DNA antibodies), scleroderma, and fibrosis of skin and liver, and the less common immune complex deposition in kidneys and glomerulonephritis.[10-12] The type of multiorgan involvement and alloantibodies seen in cGVHD patients often has not been well represented in these preclinical models. Moreover, some models do not involve conditioning regimens, whereas others rely on radiation alone. Previously, our laboratory has studied pulmonary dysfunction and cGVHD target-organ pathology in animals conditioned with high-dose cyclophosphamide (Cy) and lethal total-body irradiation (TBI) rescued with allogeneic BM and splenocytes.[13] The functional, physiologic, and pathologic assays demonstrated that Cy and TBI–conditioned recipients of low numbers of allogeneic T cells developed bronchiolitis obliterans (BO).[14,15] BO, characterized by airway blockade, peribronchiolar fibroproliferation, and obliteration of bronchioles, is a late-stage complication of GVHD, prevalent in 2%-3% of HSCT patients and up to 6% of patients who develop GVHD.[16] Patients diagnosed with BO have a 5-year survival rate of only 10% versus 40% in patients without BO.[14] According to the National Institutes of Health consensus criteria,[2] BO is the only single pathognomonic manifestation of cGVHD of the lung; therefore, this is a bona fide cGVHD murine model.

In the present study, we identified the presence of CD4$^+$ Th cells and B220$^+$ B cells in the airways of mice that had BO, tissue-specific antibodies from sera, and alloantibody deposition in the lung and liver of cGVHD recipients. Through studies using

Submitted July 1, 2011; accepted October 28, 2011. Prepublished online as *Blood* First Edition paper, November 9, 2011; DOI 10.1182/blood-2011-07-364414.

*A.P.-M. and B.R.B. contributed equally to this study.

An Inside *Blood* analysis of this article appears at the front of this issue.

The online version of this article contains a data supplement.

The publication costs of this article were defrayed in part by page charge payment. Therefore, and solely to indicate this fact, this article is hereby marked "advertisement" in accordance with 18 USC section 1734.

wild-type (WT), knockout, and transgenic donor cells, we conclusively demonstrate that donor alloantibody secretion is essential for BO generation, providing a preclinical model in which to test interventional and prophylactic approaches for cGVHD.

The mainstay of treatment of cGVHD and BO is anti-inflammatory therapy. Corticosteroids are contained in many of the current regimens but are still associated with a high rate of progressive airway obliteration and subsequent mortality.[17] Treatment of steroid-refractory cGVHD patients with rituximab, a B cell–depleting anti-CD20 mAb, has shown a beneficial role in resolution of autoimmune disorders such as systemic lupus erythematosus and rheumatoid arthritis,[18] as well as cGVHD.[19-22] Aggregate analysis of 6 trials of steroid-refractory cGVHD showed overall response rates of 29%-36% for oral, hepatic, gastrointestinal, and lung cGVHD and 60% for cutaneous cGVHD.[23]

Additional prevention and treatment strategies clearly are needed. We focused on GC formation, critical for efficient class switching and antibody secretion by mature B cells and plasma cells. Lymphotoxin-β (LTβ)–LTβ receptor (LTβR) interactions are essential for GC formation and maintenance, ensuring proper anchoring of GC B cells within the network of follicular dendritic cells (DCs) and correct GC formation. Inhibiting the GC reaction and subsequent antibody secretion has proved to be efficacious in some systemic lupus and other autoimmune models in which B cells and antibody secretion have been implicated in pathology.[18] LTβR-Ig is a novel fusion protein that binds circulating lymphotoxin and inhibits LT-LTβR signaling.[24] We show that LTβR-Ig treatment of transplanted animals susceptible to the establishment of cGVHD and BO resulted in improved lung function along with lower tissue-specific antibody levels in the sera and fibrosis of the lung and liver. LTβR-Ig represents a potential new therapy for cGVHD prevention and treatment.

Methods

Mice

C57Bl/6 ($H2^b$) mice were purchased from the National Cancer Institute. B10.BR ($H2^k$), BALB/c ($H2^d$), and B6.129S2-Igh-6tm1Cgn/J mice on a C57Bl/6 background (referred to as μMT mice) were purchased from The Jackson Laboratory. BALB/c (m+s)IgMxJhD transgenic mice[25] were bred at the University of Minnesota animal facility. Mice were housed in a specific pathogen-free facility and used with the approval of the University of Minnesota's institutional animal care committee.

BM transplantation

B10.BR recipients were conditioned with Cy on days −3 and −2 (120 $mg \cdot kg^{-1} \cdot d^{-1}$ intraperitoneally). On day −1, recipients received TBI by x-ray (7.5 Gy). Donor BM was T-cell depleted with anti-Thy1.2 mAb followed by rabbit complement. T cells were purified from lymph nodes by incubation with phycoerythrin-labeled anti-CD19 (eBioscience), followed by anti-PE beads and depletion with a magnetic column (Miltenyi Biotec). On day 0, recipients received 10×10^6 BM cells with or without allogeneic splenocytes ($0.75\text{-}1 \times 10^6$) or purified T cells ($0.33 \times 10^6$), as indicated. Weights of individual mice were recorded twice weekly. Where indicated, recipients in cGVHD groups were given murine LTβR-Ig or control murine MOPC21 provided by Biogen Idec at 200 μg per dose intraperitoneally every 3 days from days 28-52.

Pulmonary function tests

Pulmonary function tests (PFTs) were performed as described previously.[13] Anesthetized mice were weighed, and lung function was assessed by whole-body plethysmography with the Flexivent system (SCIREQ) and analyzed with Flexivent Version 5.1 software.

Frozen tissue preparation

All organs harvested were embedded in optimal cutting temperature compound, snap-frozen in liquid nitrogen, and stored at −80°. Lungs were inflated by infusion of 1 mL of optimal cutting temperature compound:PBS (3:1) intratracheally before harvest.

Histology and trichrome staining

Six-micrometer cryosections were fixed for 5 minutes in acetone and stained with H&E to determine pathology and with a Masson trichrome staining kit (Sigma-Aldrich) for detection of collagen deposition. Histopathology scores were assigned as described previously.[26] Collagen deposition was quantified on trichrome-stained sections as a ratio of area of blue staining to area of total staining by use of the Adobe Photoshop CS3 analysis tool.

Immunohistochemistry

Acetone-fixed 6-μm cryosections were immunoperoxidase stained with biotinylated mAbs for CD4, CD8, and B220 (BD Pharmingen).[26] Stained sections were examined under 200× magnification, and images were captured with an Olympus BX51 microscope. Antibody-binding–positive cells were quantified by counting a 100-mm^2 area for liver or obtaining a ratio of positive to total cells in a 100-mm^2 area for lung.

Immunofluorescence

For Ig deposition, 6-μm cryosections were fixed with acetone, blocked with horse serum, and stained with either FITC-labeled anti–mouse Ig (BD Pharmingen) or goat anti–mouse IgM, goat anti–mouse IgG1, goat anti–mouse IgG2b, goat anti–mouse IgG2c, or goat anti–mouse IgG3, followed by FITC-labeled donkey anti–goat Ig (Jackson ImmunoResearch). For detection of tissue-specific serum antibodies, fixed cryosections of organs from a naive B10.BR mouse were incubated with sera from the BM-transplanted (BMT) recipients. Sections were incubated with FITC-labeled anti–mouse Ig. Confocal images were acquired on an Olympus FluoView500 confocal laser scanning microscope at 200× magnification, analyzed with FluoView 3.2 software (Olympus), and processed with Adobe Photoshop CS3 Version 9.0.2. Antibody deposition was quantified by scoring sections by use of a scale from 1-3.

GC detection

Fixed 6-μm spleen cryosections were stained with rat anti–mouse VCAM1 followed by Cy3-labeled goat anti–rat, FITC-labeled rat anti–mouse IgM, and biotinylated peanut agglutinin (Vector Laboratories), followed by streptavidin Cy5. Confocal images were obtained as described in "Immunofluorescence."

Statistical analysis

Survival data were analyzed by life-table methods, and actuarial survival rates are shown. Group comparisons were made by log-rank test statistics. Group comparisons of cell counts and flow cytometry data were analyzed by Student *t* test.

Results

Multiorgan pathology with fibrosis in Cy/TBI recipients experiencing cGVHD

B10.BR mice were conditioned with Cy/TBI and received either BM alone (BMT control group) or BM with low-dose splenocytes to induce a chronic alloresponse not associated with early post-BMT mortality. Weight curves (Figure 1A) and 2-month survival

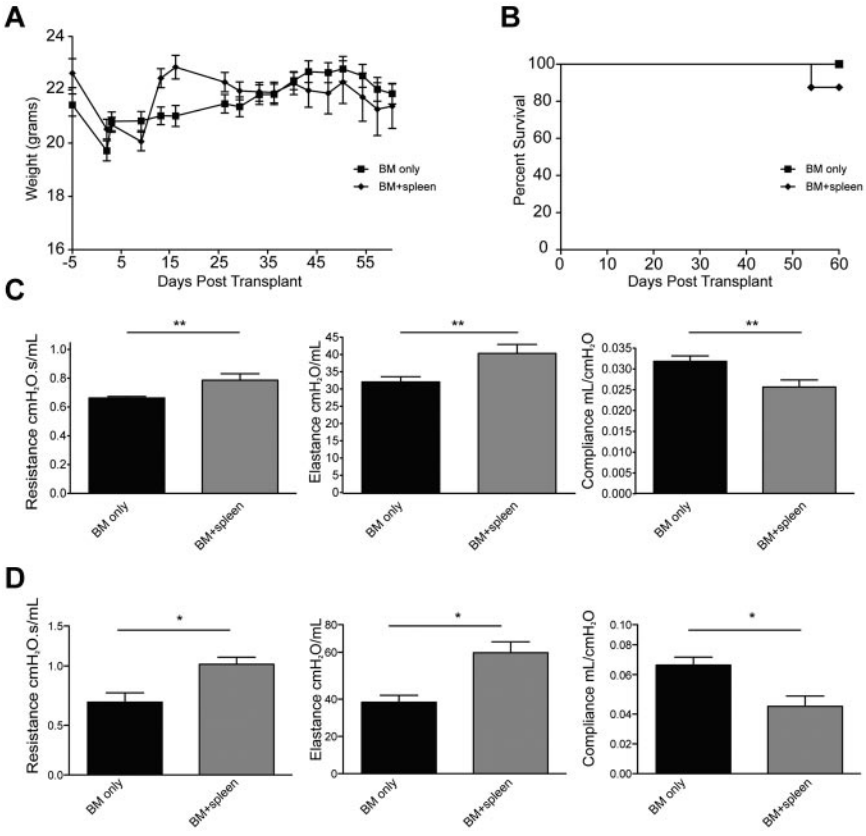

Figure 1. Allogeneic transfer of BM and low concentrations of splenic cells in hosts treated with Cy/TBI-caused cGVHD and BO. B10.BR mice treated with 120 mg · kg^{-1} · d^{-1} Cy (day −3, −2) and lethally irradiated (day −1) were transplanted with BM alone or BM plus 0.75-1 × 10^6 splenocytes from C57Bl/6 mice. n = 10 mice/group. Weights of the animals (A) and survival (B) were tracked up to 60 days after transplantation. PFTs were performed on anesthetized animals at day 60 (C) and day 28 (D) after transplantation. Animals were artificially ventilated, and resistance, elastance, and compliance were measured as parameters of distress in lung function in animals receiving low-dose splenocytes or T cells. Representative data from 3 individual experiments. $^{**}P < .01$.

rates were ≥ 90% and were comparable between groups (Figure 1B). On day 60, PFTs in the cGVHD group (Figure 1C) demonstrated lung dysfunction consistent with BO.[13] The PFTs showed an increase in airway resistance, which correlated with lung constriction, increased elastance, and decreased compliance, which signifies increased stiffness or rigidity of the lungs. These data simulate BO manifestations in cGVHD patients.[16] A decrease in pulmonary function and increased pathology was noticed as early as 28 days after transplantation (Figure 1D; supplemental Figure 2, available on the *Blood* Web site; see the Supplemental Materials link at the top of the online article). Therefore, this system is a bona fide model of cGVHD based on extrapolation of the National Institutes of Health's consensus criteria for cGVHD diagnosis in patients.[2]

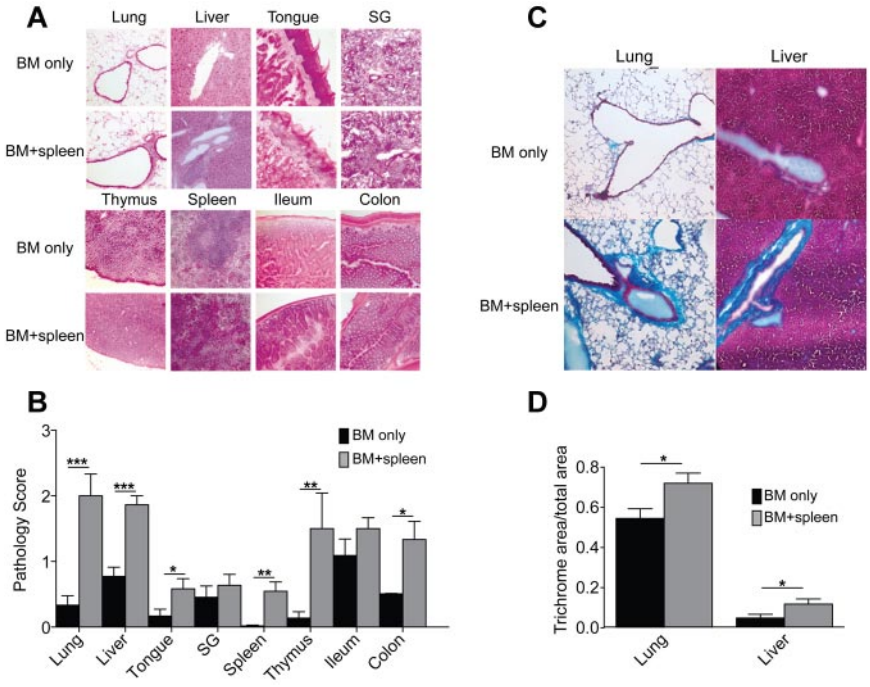

Figure 2. Multiorgan disease in mice with cGVHD; immune infiltration and collagen deposition. (A) Tissues (lung, liver, tongue, salivary glands [SG], thymus, spleen, ileum, and colon) were harvested at day 60 after transplantation and stained with H&E to determine pathology. Bright-field images were captured at 100× magnification with an Olympus BX51 microscope. (B) Inflammation, immune infiltration, and parenchymal changes were scored with a cumulative scoring system used previously.[26] (C) Collagen deposition was determined with a Masson trichrome staining kit; blue indicates collagen deposition. (D) Collagen deposition was quantified as a ratio of blue area to total area of tissue. Quantification was performed with the analysis tool in Photoshop CS3. Data from 2 individual experiments were pooled to obtain pathology scores; n = 12. $^{*}P < .05$; $^{**}P < .01$; $^{***}P < .005$.

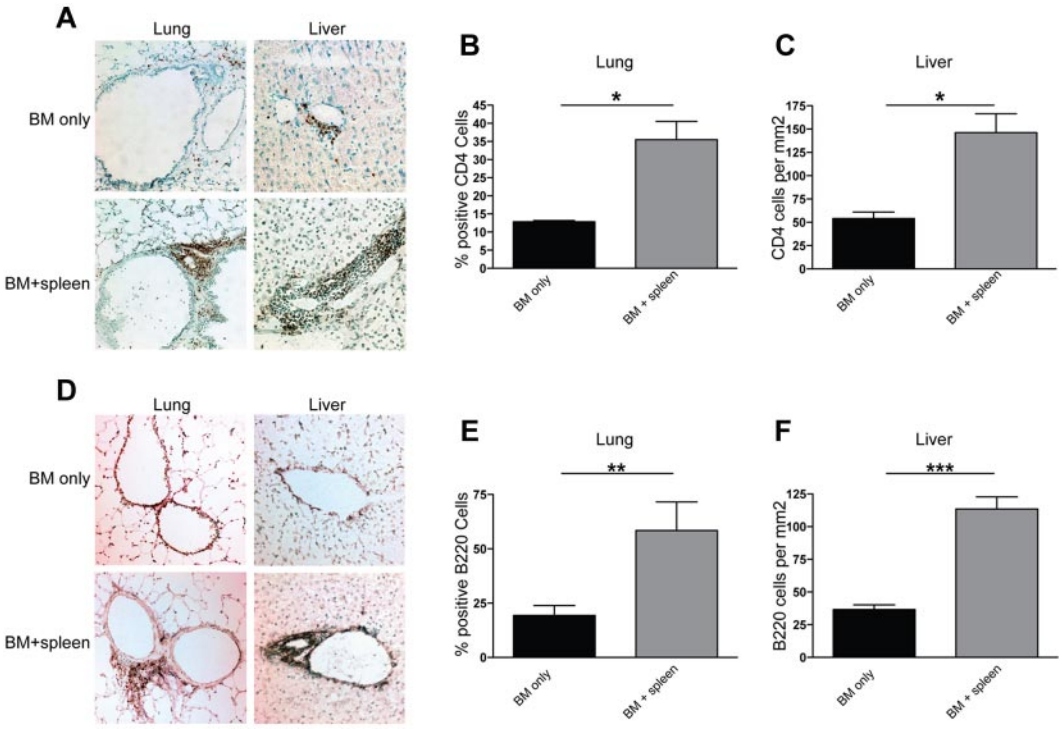

Figure 3. CD4$^+$ T-cell and B220$^+$ B-cell infiltration is seen in lungs and livers of transplanted animals. Liver and lung tissues were harvested at day 60 after transplantation from animals receiving BM only and BM plus splenocytes (BM + spleen) and analyzed by immunohistochemistry and methyl blue counterstaining. Representative images from 3 individual experiments are shown for CD4 (A) and B220 (D). Images were captured with a bright-field microscope at 200× magnification. For lung, infiltration was quantified by obtaining a ratio of CD4$^+$ (B) or B220$^+$ (E) cells to total cells in a 100-mm^2 field of view under the microscope. Shown is an average of the count from 4 representative fields. For liver, CD4 (C) and B220 (F) cell infiltration was quantified by counting the number of antibody binding–positive cells and obtaining an average of counts from 4 representative fields. n = 6. *$P < .05$; **$P < .01$; ***$P < .005$.

The cGVHD group displayed multiorgan pathophysiology consistent with cGVHD (Figure 2A-B). Lung histology showed peribronchiolar infiltration and cuffling denoting the onset of obliteration of the bronchioles (Figure 2A). Many animals displayed distal pathology in the lungs, including protein exudation, macrophage infiltration, and the start of tissue remodeling (supplemental Figure 1). Lung pathology scores were significantly higher in the cGVHD group than in BMT controls (Figure 2B). In the liver, perivascular infiltration was observed surrounding the bile duct and extending into the parenchyma (Figure 2A), which resulted in a significant increase in the pathology score in the cGVHD versus the BMT control animals (Figure 2B). Mice with higher pathology scores also had necrotic foci of cells in the parenchyma proper.

Because patients with cGVHD may also have oral mucosal involvement, histopathology of the tongue and salivary glands was examined. Areas of infiltration, inflammation, and abscess formation were observed on the tongue near the taste receptors (Figure 2A). The pathology score was significantly higher, albeit modest in magnitude, in the cGVHD group than in the BMT-only controls (Figure 2B). Salivary glands displayed perivascular infiltration; however, this infiltration was also seen in the BMT controls, which suggests changes resulting from the conditioning (Figure 2A).

The thymus, known to be involved in human cGVHD,[27] displayed necrotic foci and destruction of stromal matrix, which resulted in a significantly higher cGVHD pathology score. The spleen had abnormal architecture similar to the thymus, albeit only modest differences were seen in the pathology score. The colon displayed moderate pathology in the cGVHD cohorts, although it was not as extensive or invasive as in acute GVHD (aGVHD) models. The ileum displayed the mild pathology seen in both the cGVHD and the BMT group, which suggests the role of pretransplantation conditioning.

cGVHD has been characterized as a fibroproliferative disease, and therefore, collagen levels were quantified by trichrome staining. The lung and liver (Figure 2C-D) both displayed a significant increase in collagen deposition around bronchioles and blood vessels. The organization of the collagen surrounding the bronchioles and blood vessels is highlighted and demonstrates that the increase in collagen was localized to specific structures and not uniformly distributed throughout the lungs and liver (Figure 2C). Fibrosis patterns in tongue and salivary glands were somewhat more variable between individual mice within a group, and trichrome staining was not increased significantly compared with the BMT controls (data not shown).

Overall, Cy/TBI conditioning followed by the transfer of a low-splenocyte infusion reproduced the pathology of cGVHD. It was distinguished from aGVHD by the absence of significant weight loss early and overall mild losses later after transplantation, BO, involvement of the oral mucosa, and fibrosis in cGVHD target organs. Although pathology and fibrosis in the lung have been observed previously,[13] documented reports of pathology in the other organs have not been evaluated.

CD4$^+$ T-cell and B-cell infiltration and alloantibody deposition in cGVHD target organs

We sought to determine the potential etiopathogenic mechanisms associated with cGVHD. We focused on the lung and liver as the two most severely affected cGVHD organs denoted by obstructive PFTs and the presence of fibrosis. CD4$^+$ T-cell infiltration was

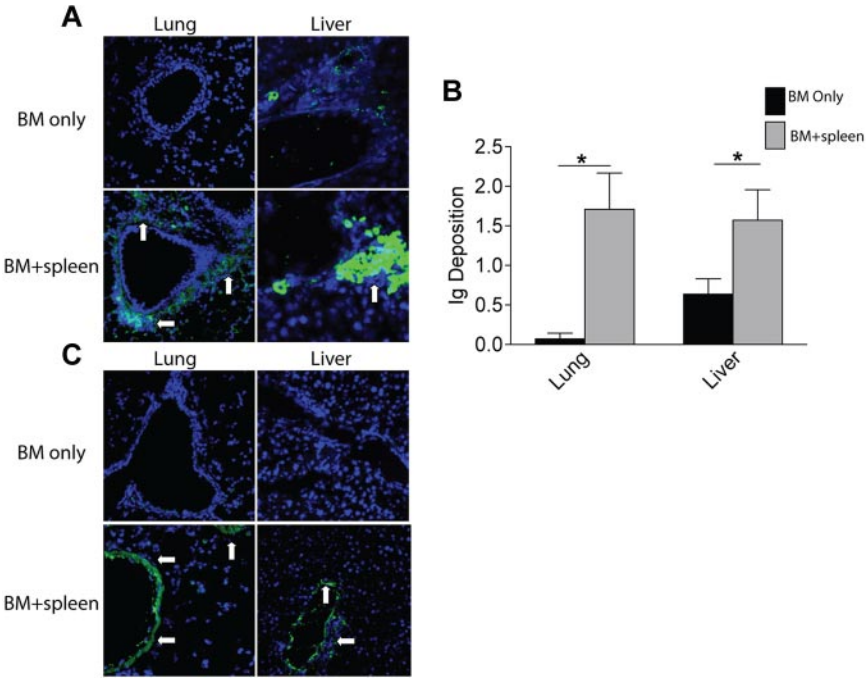

Figure 4. Antibody deposition detected in target areas of lung and liver in diseased animals. Six-micrometer sections of frozen lung and liver tissues harvested at day 60 after transplantation were analyzed by immunofluorescence. Tissues were incubated with FITC-conjugated anti-mouse Ig. (A) Representative images for lung and liver from 3 individual experiments. n = 8. (B) Ig deposition was quantified on a 0-3 scale to determine the amount of antibody in the tissues. (C) Serum from animals given BM only and animals given BM plus splenocytes was collected at day 60 after transplantation and incubated with healthy B10.BR lung and liver tissue followed by FITC-conjugated anti-mouse Ig to detect the presence of tissue-specific antibodies in the serum of diseased animals. White arrows depict areas of Ig deposition. Fluorescence was detected with an Olympus FluoView 500 confocal laser scanning microscope at a magnification of 200×.

observed in peribronchiolar areas in the cGVHD group but not in BMT-only controls (Figure 3A). The liver displayed substantial infiltration in the perivascular areas (Figure 3A) and, for some recipients, into the parenchyma (not shown). Because of the degree of lung inflation influencing the distribution of cells, percentages of lymphocytes were quantified in the lung versus the total number. The number of $CD4^+$ T cells in the lung (Figure 3B) and the liver (Figure 3C) was significantly higher in the cGVHD group than in the BMT-only control group, consistent with other models in which $CD4^+$ T cells could be found in cGVHD organs.[10] There was only minimal infiltration of $CD8^+$ T cells in both groups (data not shown). $B220^+$ B-cell infiltration in the lung and liver (Figure 3D) was seen in a pattern similar to that of $CD4^+$ T cells. A significant increase in total $B220^+$ B cells in the lung and liver was seen in the cGVHD group compared with the BMT controls (Figures 3E and 3F, respectively). Salivary glands and the tongue had only minimal $B220^+$ B-cell infiltration (data not shown). Taken together, the pathology in the lung and liver was associated with $CD4^+$ T-cell and B-cell infiltration.

We hypothesized that B cell–secreted antibodies might play a role in cGVHD pathology and determined whether antibody deposition could be observed in cGVHD organs on day 60 after transplantation. The lung and liver had deposits of mouse Ig within surrounding areas of infiltration and pathologic effects (Figure 4A). There were peribronchiolar deposits and perivascular deposits in both organs. Quantification of Ig deposition in the lung and liver (Figure 4B) revealed higher levels in the cGVHD group than in the BMT controls. The predominant Ig type was IgG2c in the lung and liver (supplemental Figure 3 and data not shown).

To determine whether circulating anti-host tissue-reactive antibodies were present, sera from transplanted animals were incubated with tissues from a naive B10.BR mouse and then probed with fluorochrome-labeled anti-mouse Ig (Figure 4C). Fluorescence was evident in the perivascular areas in lung and liver and in the peribronchiolar area in lung. These results indicate that circulating host tissue-reactive antibodies may contribute to cGVHD pathology.

cGVHD pathogenesis requires the production and secretion of anti-host reactive antibodies

To further test our hypothesis that B cells and secreted alloantibodies play a causative role in establishment of cGVHD, we used donor μMT mice that do not have membrane-bound IgM and are deficient in mature B cells (Figure 5). To limit the contribution of donor B cells and avoid any issues related to defective regulatory T-cell dysfunction reported in μMT mice, Cy/TBI-conditioned recipients received WT or μMT BM with or without supplemental WT T cells (0.33×10^6). Recipients of WT BM plus supplemental WT T cells versus low-dose splenocytes had comparable survival and weight and had significant increases in resistance and elastance, with a lowering of compliance that was characteristic of BO. When recipients of B cell–deficient BM and WT T cells were compared with mice with cGVHD that received WT BM with WT T cells, PFTs demonstrated lower resistance, elastance, and higher compliance (Figure 5A). Control recipients of WT compared with μMT BM had comparable parameters. Recipients of B cell–deficient BM with WT T cells had resistance and elastance comparable to that of recipients of B cell–deficient BM without supplemental T cells. Thus, donor allogeneic T cells and BM-derived mature B cells are required for BO generation.

In contrast to recipients of WT BM plus T cells versus BM alone, there were no significant differences in the histopathology scores of lung and liver between mice given μMT BM plus T cells and those given WT BM (supplemental Figure 4). Of note, although lymphocyte infiltration and inflammation were observed in recipients of μMT BM and T cells, there was no destruction of the bronchioles or bile ducts, and the degree of fibrosis mirrored the extent of pathologic injury (Figure 5B). The somewhat higher amounts of fibrosis in recipients of μMT BM with or without WT T cells may be due to the known Treg defect in μMT mice,[28] which then could have failed to control the inflammatory response in the lung and liver in cGVHD mice, offsetting in part the effect of B-cell deficiency. Moreover, Ig was not deposited in the lung or liver of

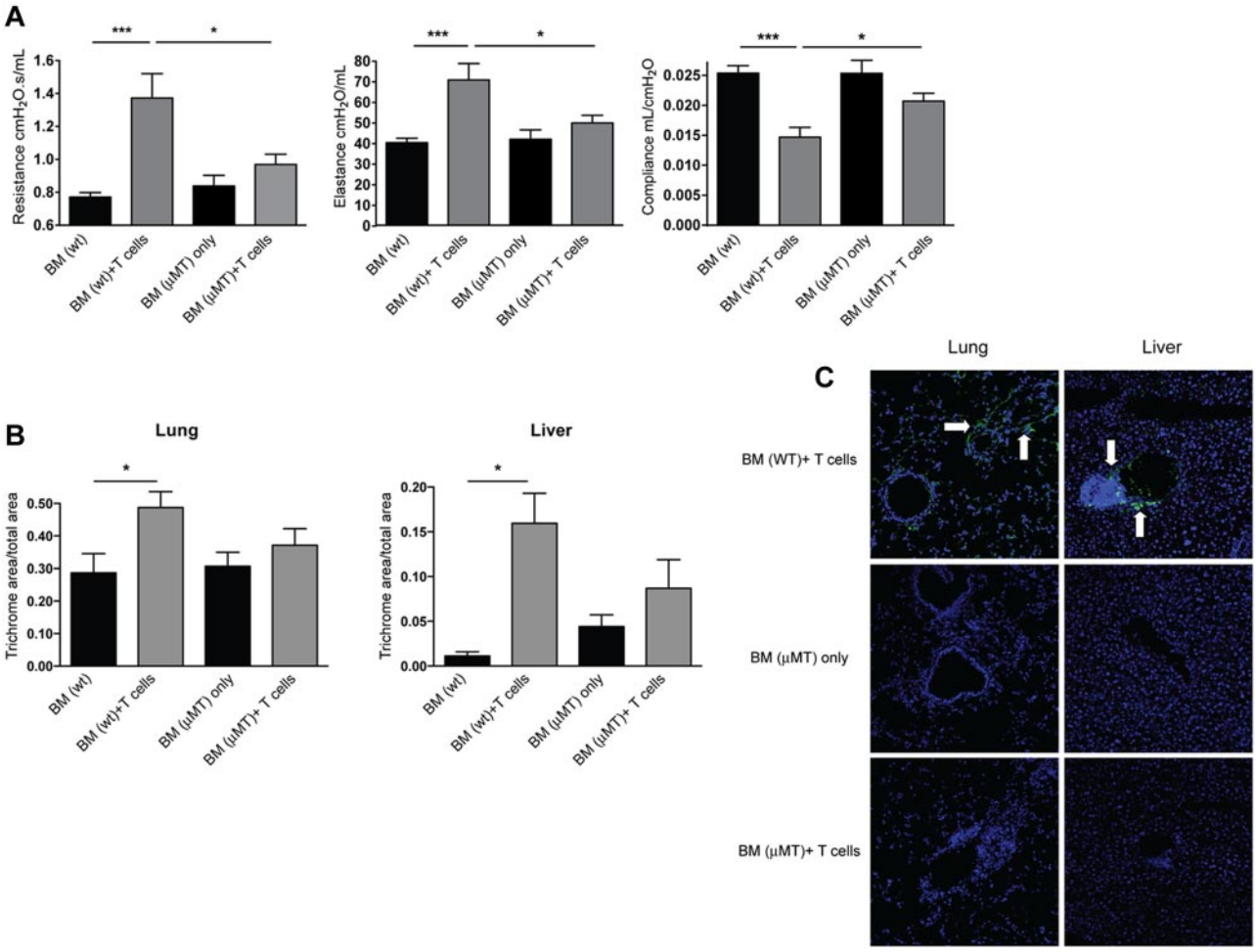

Figure 5. Animals receiving B cell–deficient BM show a decrease in pathology. B10.BR recipients were transplanted with WT BM or BM from μMT knockout mice with or without WT T cells. (A) At 60 days after transplantation, mice were anesthetized and artificially ventilated to measure pulmonary function parameters. (B) Collagen deposition was quantified from trichrome-stained samples as a ratio of blue area to total area of tissue. Quantification was performed with the analysis tool in Photoshop CS3. (C) Lung and liver tissues were harvested, and 6-μm frozen sections were stained with FITC-conjugated anti–mouse Ig for antibody deposition within the tissues. White arrows denote areas of Ig deposition. Images shown are representative images of 3 individual experiments; n = 4. *$P < .05$; ***$P < .005$; $P = .4066$ for lung BM (μMT) only vs BM (μMT) + T cells; $P = .2860$ for liver BM (μMT) only vs BM (μMT) + T cells.

mice that received μMT BM and T cells (Figure 5C), findings that correlated with results of PFTs.

We cannot exclude the possibility that antibody deposition is a bystander in the disease process and that the critical pathogenic mechanism is the APC function rather than Ig capacity of activated B cells. To distinguish between these two fundamental mechanisms, we used (m+s)IgMxJhD BALB/c donors. These mice are capable of generating membrane-bound IgM and secreting IgM, but they produce and secrete ≥ 100-fold less antigen-specific IgG than similarly immunized WT controls.[29] They also do not appear to have a regulatory T-cell defect like the μMT mice (supplemental Figure 5). Recipients were given WT BM or transgenic BM alone or with WT splenocytes. Day 60 PFTs in conditioned B10.BR recipients of (m+s)IgMxJhD BM and WT splenocytes had significantly lower lung resistance and elastance and higher compliance than recipients of WT BM with splenocytes (Figure 6A). These data indicate that the lack of IgG alloantibody secretion by donor BM-derived B cells precluded the pulmonary dysfunction associated with BO. This was confirmed by staining tissues for total Ig in the lung and liver (Figure 6D). Mice given (m+s)IgMxJhD BM only and mice given (m+s)IgMxJhD BM with splenocytes both had decreased deposition of Ig surrounding bronchioles and bile ducts compared with mice transplanted with WT BM and splenocytes. Collagen deposition was significantly reduced in mice that received (m+s)IgMxJhD BM with splenocytes compared with the WT BM plus splenocytes (Figure 6B). However, infiltrating $CD4^+$ cells were still observed in the lung and liver of both mice given WT BM and splenocytes and those given (m+s)IgMxJhD BM and splenocytes (Figure 6C). These data suggest that inflammation is not regulated by Ig deposition per se, and therefore, other mechanisms (eg, chemokines) are not affected by Ig deposition. The pathogenicity of Ig deposition in adversely affecting PFTs may not be the result of changes in inflammation but rather in situ injury from complement binding to deposited alloantibody or the Ig-facilitated activation of inflammatory or resident cells in situ.

Blockade of GC formation is sufficient to prevent BO and hence cGVHD generation

Because BM-derived B-cell production and secretion of anti-host reactive antibody appear to be critical for cGVHD generation, we sought to prevent antibody production by interrupting GC formation. GCs are sites where mature B cells rapidly proliferate, differentiate, and undergo somatic hypermutation that results in the production of class-switched antibody. LTβ, produced by T and

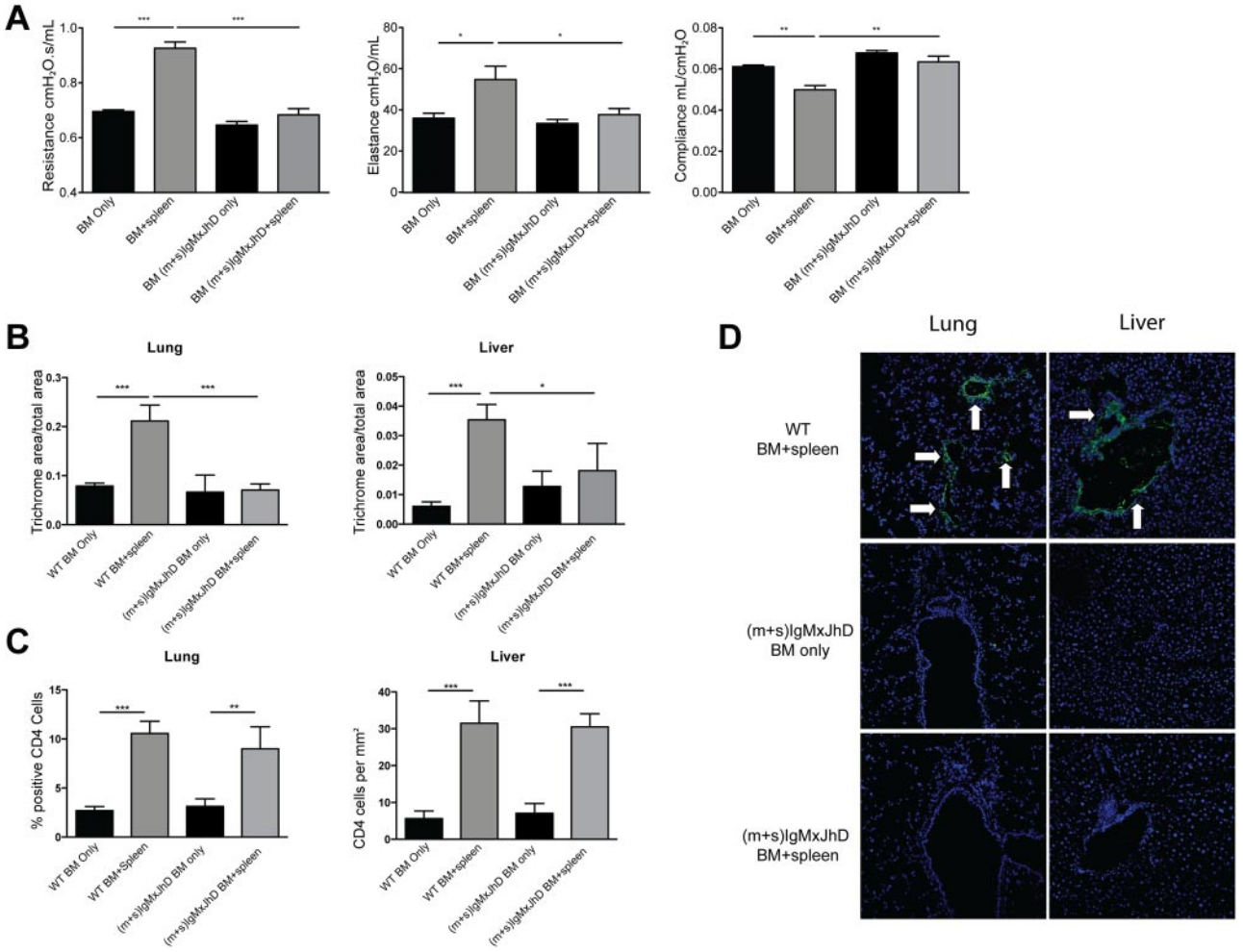

Figure 6. Secreted antibody is required for pulmonary dysfunction in animals with cGVHD. (A) B10.BR mice were transplanted with BM ± splenocytes from WT or (m+s)IgMxJhD BALB/c mice and anesthetized at day 60 after transplantation for PFTs. Resistance, compliance, and elastance were measured; n = 8. (B) Collagen deposition was quantified from trichrome-stained samples as a ratio of blue area to total area of tissue. Quantification was performed with the analysis tool in Photoshop CS3. (C) Infiltration of $CD4^+$ cells in the lung and liver of transplanted mice. (D) Lung and liver tissues were harvested, and 6-μm frozen sections were stained with FITC-conjugated anti-mouse Ig for antibody deposition within the tissues. White arrows denote areas of Ig deposition. Representative image from 2 independent experiments; n = 8. $^*P < .05$; $^{**}P < .01$; $^{***}P < .005$.

B cells, and LTβR signaling are required for proper establishment of the follicular DC network and the organizational network of functional GCs in lymphoid tissues. Given the role of LTβR signaling and our finding that the dominant Ig isotype deposited in cGVHD target organs was IgG2c, we sought to determine whether disruption of LT-LTβR signaling by infusion of a known blocking reagent, mouse LTβR-Ig fusion protein, would reduce cGVHD pathology. Recipients were treated with LTβR-Ig or control fusion protein from days 28-52 after transplantation (Figure 7). Treatment began on day 28 because of decreases in PFTs (Figure 1D) and increased GC size and frequency (supplemental Figure 8), which indicated early initiation of cGVHD. To determine the effect of LTβR-Ig on GC formation in cGVHD versus BM recipients, spleens were analyzed by immunofluorescence (Figure 7A); peanut agglutinin and IgM staining detects GC B cells, whereas VCAM-1 stains follicular DCs. Untreated and control mAb-treated mice with cGVHD pathology displayed prominent GC structures with a well-organized follicular DC network, which signifies a robust GC reaction. Mice treated with LTβR-Ig showed disrupted GC structures with an ill-formed follicular DC network. A decrease in size and frequency of GC was seen in LTβR-Ig–treated mice (Figure 7B-C).

Consistent with the finding that disruption of GC formation would diminish BO and cGVHD generation, day 60 PFTs in the cGVHD cohorts indicated that LTβR-Ig–treated but not control protein-treated recipients displayed lower resistance and elastance and higher compliance (Figure 7D). Both liver and pulmonary fibrosis was reduced by LTβR-Ig (Figure 7E). Thus, LTβR-Ig treatment given after transplantation ameliorated the development of BO and cGVHD. The pathologic scores showed that mean lung scores of mice given BM plus splenocytes plus MOPC21 were ~ 5-fold higher than those that received BM plus splenocytes plus LTβR-Ig (supplemental Figure 7), although these differences did not reach statistical significance. For the liver, recipients given BM with splenocytes treated with MOPC21 had a reduction in mean scores compared with those given BM plus splenocytes and no Ig control, thereby making it difficult to assess the extent to which LTβR-Ig was superior to MOPC21. However, we can state that recipients of BM plus splenocytes had higher scores than those of mice BM with splenocytes and treated with LTbR-Ig, indicating that the LTbR-Ig did indeed reduce the severity of pathological injury. These data are supportive of our findings that LTβR-Ig reduces cGVHD as measured by PFTs, fibrosis, Ig deposition, and

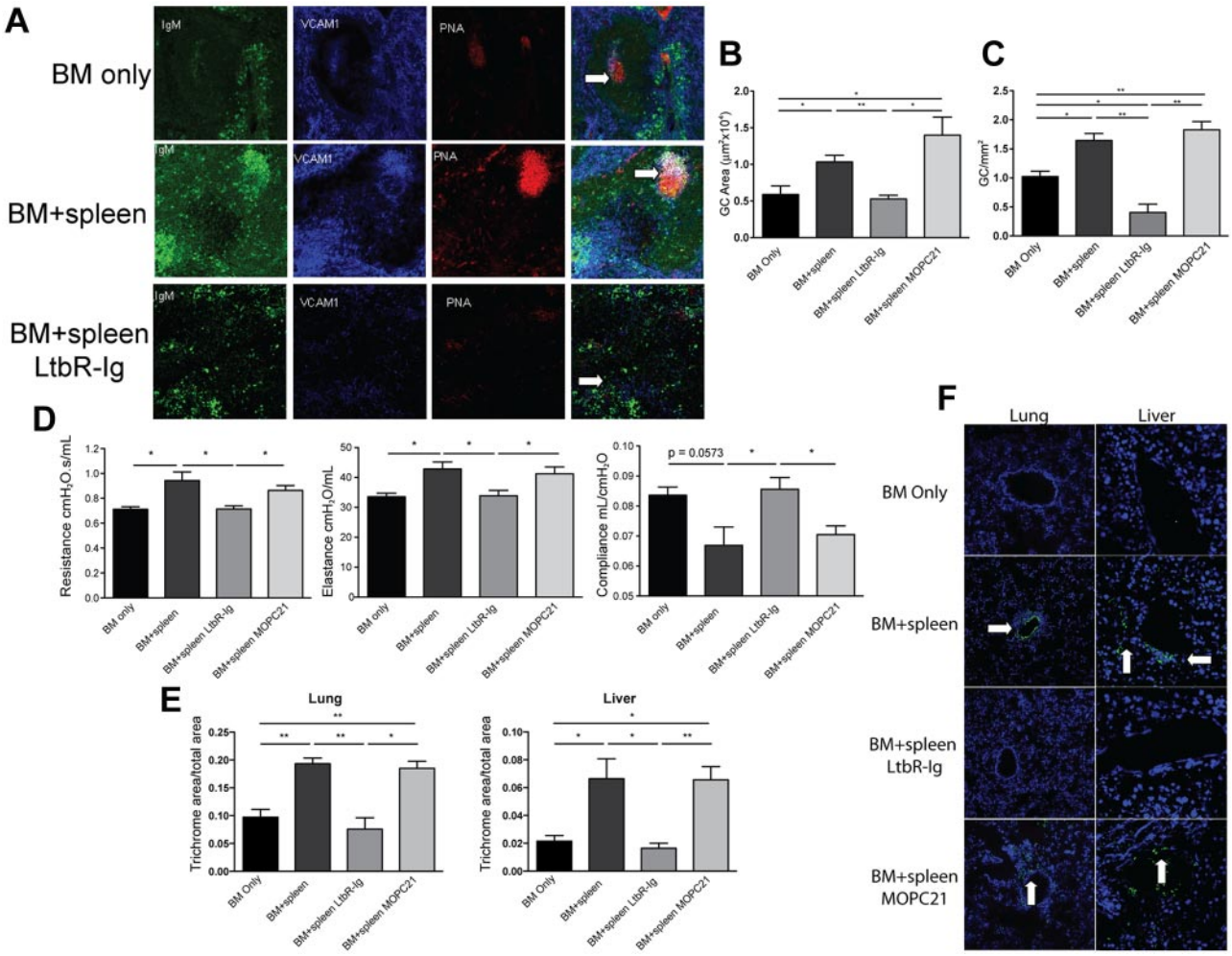

Figure 7. Disruption of GC formation by LTβR-Ig treatment reduces lung dysfunction and cGVHD organ tissue fibrosis. B10.BR recipients were transplanted as per Figure 1. A cohort of animals receiving BM + splenocytes were treated with 200 μg of murine LTβR-Ig or the control Ab, murine MOPC21, every 3 days beginning on day 28 after transplantation until day 52. (A) Spleen tissue harvested from these animals at day 60 was analyzed by immunofluorescence for GC structures. GCs were detected by colocalization of IgM (green), VCAM-1 (blue), and peanut agglutinin (red); merged images show overlap (white) to discriminate GC. White arrows highlight GC. Images were captures with an Olympus FluoView 500 confocal laser scanning microscope at 100× magnification; n = 5. (B) The size of the GC was quantified by measuring the area of peanut agglutinin staining in Photoshop C3. (C) Frequency of GCs was quantified by counting the number of GCs in 1 mm² of spleen section. (D) PFTs were performed on anesthetized animals on day 60 after transplantation to measure lung function. (E) Animals treated with LTβR-Ig and MOPC21 were examined for fibrosis in the lung and liver. (F) Presence of deposited lung and liver tissue–specific antibodies in animals treated with LTβR-Ig and MOPC21 was determined by immunofluorescence by staining with FITC-conjugated anti–mouse Ig. White arrows depict Ig deposition. Images were captured at 200× magnification and are representative of 2 individual experiments; n = 5. *$P < .05$; **$P < .01$.

GC formation, all of which showed a marked reduction in BO and chronic GVHD manifestations.

To test our hypothesis that LTβR-Ig treatment works by inhibiting antibody secretion by class-switched B cells, we assayed for the presence of host tissue–reactive antibodies in the sera of transplanted animals using a serum-binding assay. Compared with control mAb–treated recipients, sera from mice that were treated with LTβR-Ig had reduced fluorescence in the peribronchiolar area of the lung and perivascular area of the liver (Figure 7F), which indicates that LTβR-Ig but not control protein leads to a decrease in the production of anti-host reactive antibody, consistent with the improvement in PFTs.

These results suggest that B cells, via their antibody secretory capability, contribute to pulmonary dysfunction and liver pathology in animals that have cGVHD after transplantation, and interventional strategies that inhibit pathways involved in B-cell function and antibody secretion may be useful in the prevention or treatment of cGVHD.

Discussion

We report that Cy/TBI-conditioned allogeneic recipients given low splenocyte or T-cell doses developed multiorgan system pathology with fibrosis and BO pathognomonic of cGVHD of the lung. cGVHD development was associated with IgG2c deposition in the lung and liver and IgG2b in the liver, which was abrogated if the donor BM was deficient in mature B cells or incapable of producing anti-host reactive IgG. Robust GC formation was seen in mice with cGVHD. By disrupting GC formation with LTβR-Ig, BO was reduced. Together, these data indicate that GC formation and IgG secretion by donor BM-derived mature B cells are necessary for cGVHD pathology.

The use of Cy, which exacerbates TBI-induced glutathione redox reactions in the lung,[30] along with sublethal doses of donor T cells (to avoid aGVHD) favored the generation of cGVHD. The histologic changes in this model were similar to the findings in

human cGVHD.[4] The lungs showed peribronchiolar and perivascular cuffing and infiltration of the airway epithelium. The pathology appeared predominantly bronchiolar, with some alveolar involvement. Completely occluded bronchioles are observed in 20% of the animals in this model.[13] The pattern of inflammation along with increased collagen deposition surrounding nonobliterated bronchioles was similar to the pathology that defines occluded bronchioles in humans.[31] The liver had inflammation and lymphocytic infiltration, along with collagen deposition in the vascular epithelium and around the bile ducts and apoptotic foci in the parenchyma. Salivary gland pathology is an important clinical manifestation of cGVHD; patients suffer from xerostomia, histopathologic analysis shows mononuclear infiltration and fibrosis,[32,33] and salivary gland injury is a known finding in a minor mismatch mouse model of cGVHD.[34] The parotid and submandibular salivary glands displayed lymphocytic infiltrates in both the BM and cGVHD groups, likely because of transplantation conditioning. In the tongue, there was a quantifiable difference in the histology; however, the extent of inflammation and infiltration was mild to moderate and isolated to small regions of the epithelium. Similar profiles of fibrosis were seen in the tongue and salivary glands for both control and cGVHD groups, which suggests that the oral mucosa did not manifest cGVHD or that the kinetics were delayed compared with the liver and lung. The absence of any inflammatory or fibrotic changes in the skin differs from some other models in which the predominant feature is scleroderma (reviewed in Sarantopoulos et al[8]). This systemic histologic profile reinforces the observation that in mice, as in humans, the pathologic manifestations of cGVHD are heterogeneous.

The role of $CD4^+$ T cells in both aGVHD and cGVHD has been well chronicled. We also observed the presence of $CD4^+$ T cells in the zones of inflammation in both lung and liver of affected animals. A significantly higher number of $B220^+$ B cells were found clustered with the $CD4^+$ T cells, which sets up a situation in which $CD4^+$ T-cell help for B-cell alloantibody production might occur in situ in cGVHD target organs. Although donor $CD8^+$ T-cell involvement has been reported to play a causative role in airway obliteration after BMT,[31] we did not observe a higher incidence of $CD8^+$ T cells in the inflamed and affected regions of the lungs or livers (data not shown). We detected antibody deposition in the target areas of lung and liver, which confirms the involvement of B cells. Examining sera from these animals, we detected the presence of lung and liver tissue–specific antibodies. Further characterization is required to identify whether these antibodies are donor-versus-host alloreactive or autoreactive because of a breakdown in the tolerance processes after BMT. Thus, it appears that the tissue modifications and fibrosis stem from a coordinated $CD4^+$ T-cell and B-cell response.

Alleviation of physiologic and histologic symptoms in animals that received B cell–deficient BM compared with WT BM confirms the requirement of B cells for lung dysfunction and inflammation and fibrosis in the lung and liver. These animals displayed a less restrictive pulmonary physiology and a lower incidence of occluded and fibrotic airways, which signifies healthier lungs. The liver displayed less intensive inflammation and fibrosis, consistent with a study that reported attenuated liver fibrosis after toxin injury in B cell–deficient mice.[35] The use of (m+s)IgxJhD mice that can only secrete IgM and not IgG[29] as donors excluded the capacity of donor B cells to facilitate cGVHD manifestations because of enhanced pathogenic antibody production as a product of class switching and affinity maturation. B cells and follicular DCs have intact APC function, although the B-cell receptor repertoire is restricted because of the use of a fixed IgM-Vh region.[36] On day 60 after transplantation, the lung physiology showed a significantly healthy phenotype compared with the cGVHD group. The lack of secreted antibody other than IgM alleviated the functional consequences of cGVHD in the lung. These data indicate that either IgG secretion is necessary for pathogenicity or a full B-cell receptor repertoire is required to promote disease. The repertoire in turn could control the quality and specificity of the alloreactive antibodies secreted, as well as any required APC function of specific B cells for pathogenic $CD4^+$ T cells. Further work will be required to dissect these two related possibilities.

Given a role for IgG antibodies, we propose that alloantibody binding to cGVHD organs could enable tissue destruction and modifications via donor cell–mediated antibody-dependent cellular cytotoxicity or antibody-dependent phagocytosis. Alternatively, the pathology could be defined by the specific function of these secreted antibodies. For example, elevated titers of anti-PDGFR antibody have been detected in sera of patients with extensive cGVHD.[37] This antibody has been implicated in a signal transduction pathway that ultimately leads to the induction of type 1 collagen production and fibrosis.[5] Pathogenic antibody production, therefore, is likely to be an important inducer of cGVHD, and targeting this specific function of the B cells is an attractive strategy to prevent or treat early manifestations of cGVHD.

Treatment of cGVHD with the anti-CD20, B cell–depleting antibody rituximab ameliorates some manifestations of cGVHD, but it rarely results in complete remission of cGVHD.[5] In studies using mice and monkeys, it has been shown that rituximab treatment is more successful in removal of B cells from the blood than from spleen and lymph nodes.[38,39] GC B cells display lower susceptibility to rituximab-mediated clearance, probably because they reside in a nonoptimal environment for antibody-based depletion.[18] Our observation that GC B cells are critical to the development of cGVHD suggests that agents that are more effective at disrupting the GC might be more useful clinically. We are unaware of the use of rituximab in a systemic fashion to determine the effects on BO in cGVHD patients. Such studies would require patients with the same duration of onset and severity of BO. To the best of our knowledge, the relative number and frequency of infiltrated B cells have not been evaluated in the secondary lymphoid organs of patients with cGVHD, although high GC formation could occur because of increased BAFF levels.[7,40]

GCs are specialized regions found in secondary lymphoid organs in which activated B cells undergo diversification and affinity maturation that result in differentiation into both memory B cells and long-lived plasma cells that produce high-affinity, antigen-specific, class-switched antibodies. GCs are required for a sustained humoral immune reaction to alloreactive antigens but also could result in the production of autoreactive antibodies and a dysregulated autoimmune response, which might be relevant in patients who have cGVHD symptoms.[41] Follicular B cells express LT-$\alpha\beta$, whereas follicular DCs express LTβR. One of the important consequences of the LT-LTβR interaction between these cells is the proper positioning of GC B cells and establishment of GC architecture. LT-LTβR signaling also enhances the follicular DC–B cell interactions by up-regulating expression of adhesion factors such as VCAM-1 on the follicular DCs. Inhibition of this interaction by use of the LTβR-Ig fusion protein prevents GC formation.[42]

Treatment with LTβR-Ig had a direct effect on the symptoms of cGVHD, at least in part by blocking GC formation. These effects included an alleviation of pulmonary dysfunction. There was also a decrease in tissue-specific Ig levels in the sera. This confirms that

inhibition of antibody secretion from post-GC B cells and plasmablasts elicits a positive response in animals that have pulmonary GVHD. The presence of IgG2c deposits in lung and liver further supports the notion that successful GC reactions that result in class switching are an important parameter in establishing lung and liver pathology. The fusion protein could work as a potential therapeutic agent for GVHD by causing a breakdown in GC architecture, resultant antibody production, and conversion of B cells into memory cells and plasmablasts.

LTβR-Ig blocks both LTαβ and LIGHT, which is expressed on activated T cells and on B cells.[42] LIGHT has been demonstrated to have a role in the fibrosis, smooth muscle hyperplasia, and airway hyperresponsiveness associated with two murine models of chronic asthma. Pharmacologic inhibition of LIGHT resulted in better lung function, and this was linked to the reduced production of TGF-β and IL-13, cytokines involved in airway remodeling after injury.[43] The efficacy of LTβR-Ig as a cGVHD interventional strategy may be the result of multiple mechanisms of action, including disruption of GCs and antibody production.

In summary, we have observed a requirement for B cells in development of cGVHD symptoms in lung and liver in a myeloablative conditioning model of allogeneic HCST. B cells, presumably via pathogenic antibody secretion by products of the GC reaction, including long-lived antibody-forming cells, play a causal role in modulating the physiology of the lung and pulmonary dysfunction. Our studies have therefore identified important immunologic processes that are involved in cGVHD and indicate that LTβR-Ig could be a potential clinical interventional strategy for prevention and therapy of cGVHD.

Acknowledgments

The authors thank Dr Qing Zhou and Dr Christine Goetz for their technical assistance and discussions. They acknowledge the use of the confocal microscope made available through a National Center for Research Resources Shared Instrumentation Grant (#1 S10 RR16851).

This work was supported in part by National Institutes of Health grant P01 CA142106-06A1.

Authorship

Contribution: M.S. designed and performed experiments, analyzed data, and wrote the paper; R.F. performed experiments, analyzed data, and edited the paper; A.P. performed experiments and analyzed data; A.R., J.L.B., and M.J.S. provided reagents, designed experiments, and edited the paper; P.A.T. designed and performed experiments, analyzed data, and edited the paper; J.R., J.H.A., W.J.M., and L.L. discussed experimental design and analysis and edited the paper; and A.P. and B.R.B. designed, discussed, and analyzed experiments and edited the paper.

Conflict-of-interest disclosure: A.R. and J.L.B. are employees of Biogen Idec. The remaining authors declare no competing financial interests.

Correspondence: Bruce R. Blazar, MD, MMC 109, University of Minnesota, 420 Delaware St SE, Minneapolis, MN 55455; e-mail: blaza001@umn.edu.

References

1. Baird K, Pavletic SZ. Chronic graft versus host disease. *Curr Opin Hematol.* 2006;13(6):426-435.
2. Filipovich AH, Weisdorf D, Pavletic S, et al. National Institutes of Health consensus development project on criteria for clinical trials in chronic graft-versus-host disease, I: diagnosis and staging working group report. *Biol Blood Marrow Transplant.* 2005;11(12):945-956.
3. Socie G, Ritz J, Martin PJ. Current challenges in chronic graft-versus-host disease. *Biol Blood Marrow Transplant.* 2010;16(1 suppl):S146-S151.
4. Baird K, Cooke K, Schultz KR. Chronic graft-versus-host disease (GVHD) in children. *Pediatr Clin North Am.* 2010;57(1):297-322.
5. Kapur R, Ebeling S, Hagenbeek A. B-cell involvement in chronic graft-versus-host disease. *Haematologica.* 2008;93(11):1702-1711.
6. Fujii H, Cuvelier G, She K, et al. Biomarkers in newly diagnosed pediatric-extensive chronic graft-versus-host disease: a report from the Children's Oncology Group. *Blood.* 2008;111(6):3276-3285.
7. Sarantopoulos S, Stevenson KE, Kim HT, et al. High levels of B-cell activating factor in patients with active chronic graft-versus-host disease. *Clin Cancer Res.* 2007;13(20):6107-6114.
8. Sarantopoulos S, Stevenson KE, Kim HT, et al. Altered B-cell homeostasis and excess BAFF in human chronic graft-versus-host disease. *Blood.* 2009;113(16):3865-3874.
9. She K, Gilman AL, Aslanian S, et al. Altered Toll-like receptor 9 responses in circulating B cells at the onset of extensive chronic graft-versus-host disease. *Biol Blood Marrow Transplant.* 2007;13(4):386-397.
10. Zhang C, Todorov I, Zhang Z, et al. Donor CD4+ T and B cells in transplants induce chronic graft-versus-host disease with autoimmune manifestations. *Blood.* 2006;107(7):2993-3001.
11. Zhang Y, McCormick LL, Desai SR, Wu C, Gilliam AC. Murine sclerodermatous graft-versus-host disease, a model for human scleroderma: cutaneous cytokines, chemokines, and immune cell activation. *J Immunol.* 2002;168(6):3088-3098.
12. Chu YW, Gress RE. Murine models of chronic graft-versus-host disease: insights and unresolved issues. *Biol Blood Marrow Transplant.* 2008;14(4):365-378.
13. Panoskaltsis-Mortari A, Tram KV, Price AP, Wendt CH, Blazar BR. A new murine model for bronchiolitis obliterans post-bone marrow transplant. *Am J Respir Crit Care Med.* 2007;176(7):713-723.
14. Dudek AZ, Mahaseth H, DeFor TE, Weisdorf DJ. Bronchiolitis obliterans in chronic graft-versus-host disease: analysis of risk factors and treatment outcomes. *Biol Blood Marrow Transplant.* 2003;9(10):657-666.
15. Al-Githmi I, Batawil N, Shigemura N, et al. Bronchiolitis obliterans following lung transplantation. *Eur J Cardiothorac Surg.* 2006;30(6):846-851.
16. Chien JW, Duncan S, Williams KM, Pavletic SZ. Bronchiolitis obliterans syndrome after allogeneic hematopoietic stem cell transplantation: an increasingly recognized manifestation of chronic graft-versus-host disease. *Biol Blood Marrow Transplant.* 2010;16(1 suppl):S106-S114.
17. Dudek AZ, Mahaseth H. Hematopoietic stem cell transplant-related airflow obstruction. *Curr Opin Oncol.* 2006;18(2):115-119.
18. Browning JL. B cells move to centre stage: novel opportunities for autoimmune disease treatment. *Nat Rev Drug Discov.* 2006;5(7):564-576.
19. Ratanatharathorn V, Ayash L, Reynolds C, et al. Treatment of chronic graft-versus-host disease with anti-CD20 chimeric monoclonal antibody. *Biol Blood Marrow Transplant.* 2003;9(8):505-511.
20. Cutler C, Miklos D, Kim HT, et al. Rituximab for steroid-refractory chronic graft-versus-host disease. *Blood.* 2006;108(2):756-762.
21. Canninga-van Dijk MR, van der Straaten HM, Fijnheer R, Sanders CJ, van den Tweel JG, Verdonck LF. Anti-CD20 monoclonal antibody treatment in 6 patients with therapy-refractory chronic graft-versus-host disease. *Blood.* 2004;104(8):2603-2606.
22. Miklos DB, Kim HT, Miller KH, et al. Antibody responses to H-Y minor histocompatibility antigens correlate with chronic graft-versus-host disease and disease remission. *Blood.* 2005;105(7):2973-2978.
23. Kharfan-Dabaja MA, Mhaskar AR, Djulbegovic B, Cutler C, Mohty M, Kumar A. Efficacy of rituximab in the setting of steroid-refractory chronic graft-versus-host disease: a systematic review and meta-analysis. *Biol Blood Marrow Transplant.* 2009;15(9):1005-1013.
24. Browning JL. Inhibition of the lymphotoxin pathway as a therapy for autoimmune disease. *Immunol Rev.* 2008;223:202-220.
25. O'Neill SK, Shlomchik MJ, Glant TT, Cao Y, Doodes PD, Finnegan A. Antigen-specific B cells are required as APCs and autoantibody-producing cells for induction of severe autoimmune arthritis. *J Immunol.* 2005;174(6):3781-3788.
26. Blazar BR, Taylor PA, McElmurry R, et al. Engraftment of severe combined immune deficient mice receiving allogeneic bone marrow via in utero or postnatal transfer. *Blood.* 1998;92(10):3949-3959.
27. Chung B, Barbara-Burnham L, Barsky L, Weinberg K. Radiosensitivity of thymic interleukin-7 production and thymopoiesis after bone marrow transplantation. *Blood.* 2001;98(5):1601-1606.
28. Baumgarth N, Jager GC, Herman OC, Herzenberg LA. CD4+ T cells derived from

B cell-deficient mice inhibit the establishment of peripheral B cell pools. *Proc Natl Acad Sci U S A.* 2000;97(9):4766-4771.

29. Chan OT, Hannum LG, Haberman AM, Madaio MP, Shlomchik MJ. A novel mouse with B cells but lacking serum antibody reveals an antibody-independent role for B cells in murine lupus. *J Exp Med.* 1999;189(10):1639-1648.
30. Ziegler TR, Panoskaltsus-Mortari A, Gu LH, et al. Regulation of glutathione redox status in lung and liver by conditioning regimens and keratinocyte growth factor in murine allogeneic bone marrow transplantation. *Transplantation.* 2001;72(8): 1354-1362.
31. Crawford SW, Clark JG. Bronchiolitis associated with bone marrow transplantation. *Clin Chest Med.* 1993;14(4):741-749.
32. Imanguli MM, Atkinson JC, Mitchell SA, et al. Salivary gland involvement in chronic graft-versus-host disease: prevalence, clinical significance, and recommendations for evaluation. *Biol Blood Marrow Transplant.* 2010;16(10):1362-1369.
33. Nagler RM, Nagler A. The molecular basis of salivary gland involvement in graft-vs.-host disease. *J Dent Res.* 2004;83(2):98-103.
34. Levy S, Nagler A, Okon S, Marmary Y. Parotid salivary gland dysfunction in chronic graft-versus-host disease (cGVHD): a longitudinal study in a mouse model. *Bone Marrow Transplant.* 2000; 25(10):1073-1078.
35. Novobrantseva TI, Majeau GR, Amatucci A, et al. Attenuated liver fibrosis in the absence of B cells. *J Clin Invest.* 2005;115(11):3072-3082.
36. Anderson SM, Hannum LG, Shlomchik MJ. Memory B cell survival and function in the absence of secreted antibody and immune complexes on follicular dendritic cells. *J Immunol.* 2006;176(8):4515-4519.
37. Svegliati S, Olivieri A, Campelli N, et al. Stimulatory autoantibodies to PDGF receptor in patients with extensive chronic graft-versus-host disease. *Blood.* 2007;110(1):237-241.
38. Gong Q, Ou Q, Ye S, et al. Importance of cellular microenvironment and circulatory dynamics in B cell immunotherapy. *J Immunol.* 2005;174(2): 817-826.
39. Hamaguchi Y, Uchida J, Cain DW, et al. The peritoneal cavity provides a protective niche for B1 and conventional B lymphocytes during anti-CD20 immunotherapy in mice. *J Immunol.* 2005; 174(7):4389-4399.
40. Kuzmina Z, Greinix HT, Weigl R, et al. Significant differences in B-cell subpopulations characterize patients with chronic graft-versus-host disease-associated dysgammaglobulinemia. *Blood.* 2011; 117(7):2265-2274.
41. Gatto D, Brink R. The germinal center reaction. *J Allergy Clin Immunol.* 2010;126(5):898-907.
42. Gommerman JL, Browning JL. Lymphotoxin/LIGHT, lymphoid microenvironments and autoimmune disease. *Nat Rev Immunol.* 2003;3(8):642-655.
43. Doherty TA, Soroosh P, Khorram N, et al. The tumor necrosis factor family member LIGHT is a target for asthmatic airway remodeling. *Nat Med.* 2011;17(5):596-603.